Wharton's jelly mesenchymal stromal cells inhibit T-cell proliferation by synergistic IDO and mitochondrial transfer mechanisms

Cécile Pochon (c.pochon@chru-nancy.fr)
Université de Lorraine - Site de Nancy: Universite de Lorraine https://orcid.org/0000-0003-0277-5611
Romain Perouf
IMoPA: Ingenierie Moleculaire et Physiopathologie Articulaire
Allan Bertrand
IMoPA: Ingenierie Moleculaire et Physiopathologie Articulaire
Anne-Béatrice Notarantonio
Nancy University Hospital Center: Centre hospitalier regional universitaire de Nancy
Naceur Charif
IMoPA: Ingenierie Moleculaire et Physiopathologie Articulaire
M. De Carvalho Bittencourt
Université de Lorraine - Site de Nancy: Universite de Lorraine
Guillemette Fouquet
Imagine Institute: Institut Imagine Institut des Maladies Genetiques
Ghislaine Cauchois
IMoPA: Ingenierie Moleculaire et Physiopathologie Articulaire
Charlotte Voisin
IMoPA: Ingenierie Moleculaire et Physiopathologie Articulaire
Danièle Bensoussan
Université de Lorraine - Site de Nancy: Universite de Lorraine
Patrick Emond
iBrain: UMR 1253 Imagerie et Cerveau
Hervé Sartelet
Nancy University Hospital Center: Centre hospitalier regional universitaire de Nancy
David Moulin
Université de Lorraine - Site de Nancy: Universite de Lorraine
Natalia de Isla
Université de Lorraine - Site de Nancy: Universite de Lorraine
Maud D'Aveni
Université de Lorraine - Site de Nancy: Universite de Lorraine
Marie-Thérèse Rubio

Université de Lorraine - Site de Nancy: Universite de Lorraine

Research Article

Keywords: MSC, Wharton's Jelly, IDO, mitochondrial transfer, GVHD

Posted Date: December 20th, 2023

DOI: https://doi.org/10.21203/rs.3.rs-3655024/v1

Abstract

Background

Wharton's jelly mesenchymal stem cells (WJ-MSCs) are multipotent stromal cells derived from the umbilical cord that may have therapeutic potential in immune-related diseases. In the context of allogeneic stem cell transplantation, WJ-MSCs represent a good candidate for graft versus host disease (GVHD) prophylaxis and treatment.

Methods

Herein, we investigated the immunomodulatory mechanisms of WJ-MSCs, produced at clinical grade according to our Good Manufacturing Practice, *in vitro* and in an experimental GVHD xenogeneic mouse model.

Results

We observed that repeated injections of IFN-γ-primed WJ-MSCs increased recipient survival and reduced histological GVHD scores while transiently colocalizing with T cells. We then demonstrated that WJ-MSCs were able to inhibit T-cell proliferation *in vitro* through indoleamine 2,3-dioxygenase (IDO) and mitochondrial transfer to T cells. Our results suggest that these processes act synergistically, since IDO is needed for the optimal effect of WJ-MSC-mediated mitochondrial transfer on T-cell metabolism, which is characterized by a switch from glycolysis toward oxidative phosphorylation.

Conclusion

Overall, our data indicate that IFN-γ-primed WJ-MSCs are able to control GVHD by reprogramming the metabolism of T cells, and we report for the first time a synergistic interplay between IDO and contact-dependent mitochondrial transfer, providing new insights for the treatment of immune-related diseases.

Introduction

Allogeneic hematopoietic stem cell transplantation (allo-HSCT) is widely used to treat various malignant and nonmalignant hematologic diseases [1]. One of the most limiting factors for the success of allo-HSCT is the occurrence of acute graft-versus-host disease (aGVHD), a posttransplant disorder resulting from an immune-mediated attack on host tissues by donor T cells in the hematopoietic stem cell transplant[2]. Currently available treatments for aGVHD rely on corticosteroids and other immunosuppressive drugs, such as the JAK2 inhibitor ruxolitinib as a second-line treatment [3]. Acute GVHD remains the primary cause of transplant-related mortality, particularly because the addition of immunosuppressive drugs increases the risk of lethal infection. Therefore, new preventive and curative therapeutic approaches are needed to improve transplant outcomes [2]. Mesenchymal stromal cells (MSCs) have therapeutic potential in severe acute GVHD[4]. While the first source of MSCs used in the clinic to prevent GVHD was bone marrow[5], Wharton’s jelly’s MSCs (WJ-MSCs) are of particular interest,

considering that they can be isolated without invasive procedures and have a high expansion rate, low degree of immunogenicity and high immunosuppressive potential *in vitro* [6],[7]. Our group has developed a bank of clinical-grade cryopreserved WJ-MSCs that are authorized by the French Medicine Agency (ANSM) for adoptive allogeneic use in clinical trials [8, 9]. Several trials have now demonstrated the feasibility and excellent tolerability of WJ-MSCs injection in patients[10–12]. In the context of GVHD, phase 1/2 trials have reported encouraging results for the prevention and treatment of GVHD[6, 10, 11]. However, to increase their therapeutic efficacy, the mechanisms of action of WJ-MSCs need to be further clarified. In this study, we explored the effect of priming WJ-MSCs with IFN-γ, which has been used with MSCs from other sources to enhance their immunomodulatory effect *in vitro* and *in vivo* [13, 14], and optimized a treatment regimen using a preclinical xenogeneic GVHD model *in vivo*. We then explored the mechanisms of T-cell inhibition in both unprimed and IFN-γ-primed WJ-MSCs *in vitro* and demonstrated that IDO and mitochondrial transfer to T cells are both required for the optimal immunosuppressive effects of WJ-MSCs.

Materials and Methods

Mice and disease models

NOD. Cg-Prkdcscidll2rgtm1 WjI/SzJ (NSG) female mice were purchased from the Jackson Laboratory, maintained in an enriched environment free from specific pathogenic organisms, and used at 8 weeks of age. Xeno-GvHD was induced as previously described[11] after approval by the local Ethical Committee CELMEA 66 (APAFIS23270-2017060417575295-V10, approved on 19th June 2018). Briefly, NSG mice were irradiated using 200 cGy total body irradiation by X-ray on day − 1 followed by intravenous injection in the caudal vein of 5.10^6 human PBSCs from a healthy donor. One injection on Day 0 or repeated injections on Days 7, 14 and 21 were performed with $5x10^5$ unprimed-MSCs or $5x10^5$ IFN-γ-primed MSCs. The control group was transplanted with only $5x10^6$ human PBSCs on Day 0 and then received PBS for further injections. The survival and body weight of mice were monitored every 2 days. Chimerism was analyzed in blood cells after staining with a mouse human V500-CD45 antibody (BD Horizon). Skin, gut, liver and spleen histological analyses were performed after hematoxylin-eosin staining. The histological score for GVHD was evaluated according to previous reports [16].

WJ-MSC preparation and characterization

Clinical grade WJ-MSCs were generated as previously described[17]. Umbilical cord collection was approved by the Nancy Hospital ethics committee and French ministry of research (No DC-214-2114).

WJ-MSC production was performed under GMP conditions in α-MEM culture medium (Macopharma, France) enriched with 5% human platelet lysate (Macopharma, France). Cross sections of the cord (3 mm) were made. Each fragment was transferred one by one to a flask (TPP 90552 Dutscher), and was allowed to attach to the plastic surface for 15 minutes before the addition of α-MEM supplemented with 5% human platelet lysate. The flasks were incubated at 37°C in hypoxia (5% CO2, 5% O2). The medium

was changed after 4 to 5 days of culture. After nearly 10 days of culture, the cross sections of the cords were removed, and the medium was renewed. When the confluence of the cells reached 80%, the medium was removed, the cells were washed with PBS (Macopharma, France), trypsinization was performed for 5 min, and the cells were recovered by centrifugation and plated in new T75 flasks at a density of 3000 MSCs/cm^2. WJ-MSCs were cultured up to P2 (final product). The same culture conditions were applied for passages 1 and 2.

At the end of P2, and after trypsinization, MSCs were frozen at a concentration of $1x10^6$/ml in a final cryopreservation solution composed of 10% human albumin and 10% dimethyl sulfoxide (DMSO). MSCs were stored at -80°C and then in vapor phase nitrogen.

MSCs were thawed in a water bath at 37°C for 5 min and then washed in fresh α-MEM enriched with 5% human platelet lysate. They were transferred to T75 flasks at a concentration of 3000 viable cells/cm2 and cultured for one week in hypoxia to restore their functions after thawing.

For IFN-γ priming, recombinant human IFN-γ protein (285-IF-100, Biotechne) was added at 100 ng/ml for 48 hours before *in vivo* administration or *in vitro* functional tests.

The WJ-MSC phenotype was analyzed with the MSC Phenotyping Kit (human, 130-095-19, Miltenyi Biotec) and with the following monoclonal antibodies (mAbs): CD80-FITC (clone 2D10.4, eBioscience), CD86-PE (clone IT2.2, eBioscience), CD209-APC (clone eB-h209, eBioscience), CD40-PE (eBioscience), HLA-DR-eFluor 450 (clone L243, eBioscience), NP1-PE (eBioscience), CD29-FITC (clone TS2/16, Fisher Scientific), VCAM-1-PE (clone STA, Fisher Scientific), mouse anti-human CD47 (clone B6-H12, eBioScience), mouse anti-human HLA-G (clone 87G, eBioscience), mouse anti-human Gal-9 (functional grade, clone 9M1-3, Fisher Scientific), and secondary goat anti-mouse Alexa Fluor 594 (Fisher Scientific), Galectin3-PE (clone M3/38 Fisher Scientific), PDL-1-APC (clone MIH1, Fisher Scientific), PDL-2-APC (Fisher Scientific), and IDO-Alexa Fluor 488 (clone 700838, Biotechne).

Tracking of WT-MSCs

For *in vivo* homing assays, WJ-MSCs were stained with Celltracker™ Deep Red Dye (Thermo Fisher) or MitoTracker Green (FM Green MitoTracker™ M7514, 488/516 nm) for 30 minutes in α-MEM without serum at 37°C 24 hours and 2 hours before injection. PBMCs were stained with Celltracker™ Blue CMAC Dye, Thermo Fisher, following instructions provided by the company, 2 hours before injection.

Proliferation assays and cell analysis:

T cells from the peripheral blood mononuclear cells of healthy donors were purified by negative selection (pan–T-cell depletion kit, Miltenyi Biotec). Purity was routinely greater than 98% (not shown). T-cell activation was performed in a 96-well round bottom plate coated with 10 µg/mL anti-CD3 mAb (clone UCHT1, R and D) and 10 µg/mL anti-CD28 mAb (clone 37407). Once labeled with CellTraceTM Violet (Thermo Fisher Scientific) at 5 µM, 50,000 T cells per well were incubated in RPMI 1640 supplemented

with 10% fetal calf serum, 10 mM N-2-hydroxyethylpiperazine-N'-2-ethanesulfonic acid buffer, 1 mM sodium pyruvate, and 100 U/mL penicillin—streptomycin (Life Technologies).

Inhibition assays were performed with an anti-human IFN-γ antibody (NIB42 RUO, BD) at 25 µg/ml, 1-methyl-L-tryptophan (Sigma—Aldrich) at 1 mM or 0.5 mM, a neutralizing monoclonal anti-PD1 antibody at 20 µg/ml, and a neutralizing monoclonal anti-human galectin-9 antibody (9S2-1, Sigma—Aldrich) at 20 µg/ml in coculture medium.

ThermoScientific® Nunc® Cell Culture Inserts in Carrier Plate System were used, with a diameter of 0.4 µm, to prevent contact between MSCs and T cells.

ELISA and MULTIPLEX:

On Day 5 of T/MSC coculture, Human LAP (TGF-Beta 1) Duoset ELISA, Human Indoleamine 2,3-dioxygenase DuoSet ELISA, and Prostaglandin E2 Parameter Assay Kits from Biotechne were used to measure TGFβ1, IDO and PGE2 levels in the supernatants. A human Magnetic Luminex Assay from Biotechne was specifically designed to measure IL-6, IL-10, soluble PDL-1, galectin-3, galectin-9, and HGF levels in the supernatants.

Tryptophan metabolites:

On Day 5 of T/MSC coculture, supernatants were frozen and sent to the UMR 1253 unit, Tours University, France. Tryptophan and its metabolites were measured with liquid chromatography coupled with high resolution mass spectrometry as described by Emond's Team [18]. Twenty metabolites were measured for each sample. IDO activity could be estimated by the ratio of tryptophan metabolites mediated by IDO (kynurenine, kynurenic acid, 3-OH kynurenine, quinolinic acid and xanthurenic acid) to other tryptophan metabolites (tryptophan, 5-OH tryptophan, tryptamine, serotonin and tryptophol).

Mitochondrial transfer analysis

WJ-MSCs were stained with MitoTracker Green (FM Green MitoTracker™ M7514, 488/516 nm) at 50 nM in α-MEM medium without serum for 30 minutes at 37°C, 2 hours before coculture with T cells. On Days 2 and 5 of coculture, the percentage of T cells that received mitochondrial material (Mito+) or did not receive mitochondrial material (Mito-) was determined by flow cytometry.

Metabolism analysis

A Seahorse XF Cell Mito Stress Kit (Agilent) was used to analyze T-cell metabolism after coculture. Briefly, 300 000 T cells were added to each well, and the oxygen consumption rate (OCR, pmol/min) and extracellular acidification rate (ECAR, mpH/min) were analyzed under basal conditions after oligomycin injection, FCCP and actinomycin A/rotenenone injection to measure basal respiration, ATP-linked respiration, and maximal respiratory capacity. The OCR/ECAR ratio was analyzed in all conditions (12 measurements per sample).

SCENITH experiments were conducted following the WJ-MSC-T-cell coculture protocol described by Argüello[19]. They developed a method for assessing protein synthesis in the presence of various metabolic inhibitors, such as oligomycin and 2DG, to measure the global metabolic activity of cells. After coculturing, T cells were harvested, counted, and then divided to be exposed to these inhibitors. Following a 15-minute incubation at 37°C, puromycin was added for a 20-minute period to bind to all actively translated proteins. Subsequently, an antibody labeled with a fluorochrome against puromycin, developed by Argüello's team, was employed to measure protein translation in T cells using flow cytometry. The GeoMFI (geometric mean fluorescence intensity) of puromycin under different conditions was utilized to determine the cell dependence on glycolysis or oxidative phosphorylation.

Statistics

GraphPad Prism 9 software was used. Comparisons between groups were performed by Student's t test or Fisher's exact test. Survival curves were compared by the log-rank test. A p value < 0.05 was considered statistically significant.

Results

Repeated injections of IFN-primed WJ-MSCs are needed to protect mice from xeno-GVHD

The WJ-MSC phenotype was analyzed by flow cytometry before cell injection in mice. Both unprimed and IFN-γ-primed WJ-MSCs expressed MSC characteristic antigens (CD90, CD73, CD105) and lacked CD45 CD34 and CD14. As previously described [20, 21], HLA-DR and CD40 expression was upregulated after IFN-γ exposure, but IFN-WJ-MSCs did not activate allogeneic T cells in coculture (data not shown). Further analyses showed that IFN-γ preexposure of WJ-MSCs upregulated the expression of PDL-1 and PDL-2 on the cell membrane and of IDO in the cytosol, while the cell surface expression of HLA-G and galectins 3 and 9 was similar between WJ-MSCs and IFN-WJ-MSCs (Fig. 1A).

To evaluate the *in vivo* immunosuppressive effects of WJ-MSCs in a xenogeneic model of allo-HSCT, we injected irradiated NOD (nonobese diabetic)–SCID (severe combined immunodeficient)–IL-2Rg−/− (NSG) mice with 5×10^6 PBMCs to induce lethal GVHD. In this model, while a single injection of 5×10^5 unprimed WJ-MSCs or 5×10^5 IFN-γ-primed WJ-MSCs (IFN-WJ-MSCs) on Day 0 did not improve overall survival compared to that of the control group (mice injected only with PBMCs) (**Fig. S1A**), the group administered repeated IFN-WJ-MSC injections on Days 7, 14 and 21 exhibited improved survival compared to that of the control group ($p = 0.0025$) and to that of the groups repeatedly injected with unprimed WJ-MSCs ($p = 0.03$) (Fig. 1B). The protective effect of IFN-γ-primed WJ-MSCs was not due to reduced human T-cell engraftment since human $CD45^+$ chimerism by Day 30 posttransplantation was similar among the three groups (Fig. 1C).

Histological signs of GVHD were observed in the liver and to some extent in the skin **(Fig S1B**) in the control group. Consistent with GVHD protection, IFN-WJ-MSC recipient mice had lower GVHD histopathological scores in the liver ($p = 0.03$) and skin ($p = 0.01$) than the GVHD control group (Fig. 1D). We tracked the homing of WJ-MSCs *in vivo* by labeling the cells with a cell tracker in transplanted mice before injection and observed their presence in the skin, lung, spleen, liver and gut. WT-MSCs were detectable twenty-four hours after injection but not at later time points and formed clusters in the lungs, as well as to some extent in the skin and spleen (Fig. 1E). In the latter, WJ-MSCs were observed in close proximity to human PBMCs (Fig. 1F).

WJ-MSCs and IFN-WJ-MSCs inhibit T-cell proliferation in vitro through IDO

We then sought to investigate the effects of WJ-MSCs and IFN-γ-primed WJ-MSCs on T-cell activation *in vitro*.

We first observed that IFN-γ-primed WJ-MSCs were more effective at inhibiting the proliferation of CD3/CD28-activated allogeneic T cells *in vitro* than unprimed WJ-MSCs (Fig. 2A). Among T cells, while WJ-MSCs had similar suppressive effects on both CD4 + and CD8 + T subtypes, a predominant inhibition of $CD4^+$ T cells was observed in the presence of IFN-WJ-MSCs (Fig. 2B). T-cell inhibition induced by WJ-MSCs was partially reversed by blocking IFN-γ in the presence of non-IFN-primed WJ-MSCs, while the reversion was not significant when WJ-MSCs had already been stimulated by IFN-γ (IFN-WJ-MSCs) **(Fig S2A**), confirming that IFN-γ enhances the immunosuppressive effects of WJ-MSCs. The reduction in T-cell proliferation was associated with the induction of T-cell apoptosis in the presence of WJ-MSCs compared to control-activated T cells alone, and this phenomenon was even more apparent with IFN-WJ-MSCs (Fig. 2C). While CD95 upregulation on the T-cell surface was observed in the presence of both WJ-MSCs and IFN-WJ-MSCs (**Fig S2B**), neither WJ-MSCs nor IFN-WJ-MSCs induced T-cell exhaustion (**Fig S2C**).

To determine the mechanisms involved in the regulation of T-cell proliferation by IFN-WJ-MSCs in comparison to unprimed WJ-MSCs, we compared regulatory molecules produced after coculture of activated T cells in the presence or absence of WJ-MSCs or IFN-WJ-MSCs. On Day 5 of coculture, in comparison to activated T cells alone, cocultures with WJ-MSCs showed increased levels of galectin-3, galectin-9, HGF, IDO, TGFβ1 and PGE2 and reduced production of IL-10 but similar levels of PDL1 despite the higher expression of membrane PDL1 and PDL2 on WJ-MSCs (Fig. 2D **and** Fig. 1A). When compared to unprimed WJ-MSCs, cocultures with IFN-WJ-MSCs displayed higher levels of IDO and galectin 9 (Fig. 2D). Suppressive activity was completely reversed in the presence of a selective inhibitor of IDO, 1 L-methyltryptophan (1 L-MT), at 1 mM **(**Fig. 2E**).** Other immunosuppressive mechanisms were excluded by adding selective inhibitors or blocking monoclonal antibodies against PD1/PDL1 **(Fig S2D)**, galectin-9 **(Fig S2E)** or all galectins to the cocultures **(Fig S2F).**

Moreover, further supporting the importance of IDO, we observed tryptophan depletion in coculture supernatants mirrored by a significant increase in the abundance of tryptophan metabolites (kynurenine and kynurenic acid), especially in the coculture with IFN-WJ-MSCs **(**Fig. 3A-B**)**, which was consistent with

higher IDO activity in IFN-WJ-MSCs (Fig. 3C). The addition of 1 L-MT at 1 mM fully restored tryptophan concentrations and inhibited IDO activity (Fig. 3A and 3C).

Both WJ-MSCs and IFN-WJ-MSCs require cell–cell contact to exert their suppressive effects (Fig. 3D). However, the absence of cell–cell contact between IFN-γ-primed or unprimed WJ-MSCs and T cells did not inhibit IDO activation (Fig. 3E), suggesting the implication of another immunosuppressive mechanism requiring cell–cell contact between WJ-MSCs and T cells.

In vitro inhibition of T-cell proliferation by WJ-MSCs involves cell–cell contact and mitochondrial transfer

Next, we explored whether WJ-MSCs could transfer mitochondrial material to activated T cells, a potential cell–cell contact-dependent mechanism recently described in this context [22]. We observed that both WJ-MSCs and IFN-WJ-MSCs could transfer their mitochondria to a median of 29.5% and 33% of activated CD4 + T cells after 2 and 5 days of coculture, respectively, in a contact-dependent manner (Fig. 4A). Mitochondrial transfer to $CD4^+$ T cells was enhanced compared to $CD8^+$ T cells with both WJ-MSCs and IFN-WJ-MSCs (Fig. 4B). Furthermore, the proliferation of CD4 + and CD8 + T cells (data not shown for CD8 + T cells) appeared to be dependent on mitochondrial transfer from WT MSCs since activated mito + T cells had a lower proliferative capacity in the presence of both WJ-MSCs and IFN-WJ-MSCs compared to that of mito-T cells (Fig. 4C). Mitochondrial transfer was totally inhibited in the absence of cell contact between WJ-MSCs and T cells (Fig. 4D), whereas IDO inhibition by 1 L-MT did not impact the rate of mitochondrial transfer from MSCs to $CD4^+$ T cells (Fig. 4E).

Altogether, these data demonstrate that the immunosuppressive effects of WJ-MSCs involve mitochondrial transfer from WJ-MSCs to T cells, particularly to $CD4^+$ T cells, in addition to IDO activity.

IDO and mitochondrial transfer act synergistically to increase oxidative phosphorylation in T cells

We then sought to determine whether IDO and mitochondrial transfer operate independently. We therefore analyzed the effect of IDO inhibition with 1 L MT on mitochondrial transfer and the proliferation of $CD4^+$ mito + versus mito- T cells.

IDO inhibition in cocultures of WJ-MSCs or IFN-WJ-MSCs and activated T cells completely restored the proliferation of mito-T cells and largely restored the proliferation of mito + T cells (Fig. 5A), suggesting a synergistic effect of the two mechanisms.

Since mitochondrial transfer is known to modulate recipient cell metabolism[22, 23], we analyzed T-cell metabolism modifications of activated T cells in the presence or absence of WJ-MSCs with or without cell contact. In comparison to CD3/CD28-activated T cells alone, the metabolism of activated T cells in contact with WJ-MSCs was characterized by reduced glycolysis and a switch toward oxidative phosphorylation under basal conditions, suggesting an increase in ATP production and T-cell maximal respiration after the addition of FCCP (Fig. 5B-C). While the inhibition of IDO or removal of cell contact

between WJ-MSCs and T cells both independently reduced oxidative phosphorylation in T cells, their combination of both IDO inhibition and cell contact removal induced a more obvious reduction of oxidative phosphorylation in activated T cells (Fig. 5B-C). Analysis of T-cell metabolism with Scenith technology confirmed that T cells transferred with WJ-MSCs mitochondria displayed a higher mitochondrial dependence and a lower glycolytic capacity when cultured with WJ-MSCs, while only a tendency was observed for IFN-WJ-MSCs (Fig. 5D-E). IDO inhibition with 1 L-MT abrogated this metabolic switch (Fig. 5D-E).

These results suggest that IDO is needed to support the T-cell metabolic switch from glycolysis to oxidative phosphorylation after receiving mitochondria.

Discussion

In this study, as reported by other groups, we confirmed that WJ-MSC priming with IFN-γ enhances their immunosuppressive effects on activated T cells *in vitro* and *in vivo* [13, 14, 24–26]. In contrast with previous works demonstrating that WJ-MSCs control T-cell activation by depleting tryptophan levels and increasing kynurenic acid levels by regulating IDO activity[14, 27–31] we report that the mechanism WJ-by which MSCs exert their immunosuppressive effects on activated T cells involves the synergism of IDO activity and mitochondrial transfer to activated T cells. We demonstrated that T cells that received mitochondrial material from WJ-MSCs displayed lower proliferation capacities and cell metabolism shifts in an IDO-dependent manner. Thus, IDO activity and mitochondrial transfer appear to be interconnected and are both needed for an optimal immunosuppressive effect of IFN-γ-primed WJ-MSCs. Metabolic analyses of activated T cells in the presence or absence of WJ-MSCs revealed that both IDO activity and mitochondrial transfer are needed to switch the metabolism of activated T cells from glycolysis to oxidative phosphorylation.

Different mechanisms by which IDO modulates T-cell metabolism have been described. Tryptophan depletion inhibits the mTOR pathway [32, 33], leading to glutaminolysis and the inhibition of aerobic glycolysis in activated T cells [32],[34]. IDO, through GCN2 kinase activation, has been described to inhibit CD4 + T-cell proliferation and downregulate key enzymes that directly or indirectly promote fatty acid synthesis, a prerequisite for CD4 + T-cell proliferation and differentiation into effector cell lineages[30]. Moreover, IDO, by degrading tryptophan, increases the activity of carnitine palmitoyltransferase I (cpt1a) and fatty acid β-oxidation in T cells [35], which is also increased by the tryptophan metabolite kynurenine [36]. These latter 2 pathways fuel the tricarboxylic acid cycle with acetyl-CoA produced in mitochondria and favor oxidative phosphorylation. Our findings demonstrate that enhanced IDO activity in IFN-γ-primed WJ-MSCs suppresses T-cell glycolysis and enhances oxidative phosphorylation. However, this T-cell metabolism conversion requires MSC mitochondrial material transfer in addition to IDO activity.

Mitochondrial transfer was described for the first time by Spees et al. in 2006 in bone marrow MSCs and fibroblasts [37]. Many reports have since described mitochondrial transfer from MSCs to many cell types (macrophages, mononuclear cells of cord blood, tumoral cells such as myeloid and lymphoid blasts,

glioblastoma and melanoma, endothelial cells, cardiomyocytes, neuronal cells, corneal epithelial cells, and T cells) [22, 38–45]. This transfer depends on Miro1, a mitochondrial Rho-GTPase, and is mainly performed through nanotunnels [48], requiring contact between cells. Court et al. recently described mitochondrial transfer from WJ-MSCs to human PBMCs *in vitro* [22]. This transfer occurred in approximately 40% of hematopoietic cells (B, T and NK cells). Consistent with our observations, the highest rate of mitochondrial transfer was found in CD4 + T cells, and the rate increased in a contact-dependent manner. In this study, artificial transfer of isolated MSC-derived mitochondria into T cells upregulated the mRNA expression of genes involved in T-cell activation and T regulatory cell differentiation[22]. This finding is consistent with another study showing FOXP3 stabilization and an increase in the suppressive function of induced Tregs after mitochondrial transfer from MSCs [45]. In our study, mitochondrial transfer and IDO activity, inducing oxidative phosphorylation, may induce the differentiation of Tregs, as suggested by a high proportion of $CD4^+$ CD25high $FoxP3^+$ T cells after coculture with WJ-MSCs (data not shown). The observed effect of mitochondrial transfer to T cells seems, however, to be donor cell source-dependent, as mitochondrial transfer from other sources, including fibroblasts or PBMCs, failed to generate a high proportion of Treg cells [22].

In mice, only repeated injections with IFN-γ-primed WJ-MSCs significantly decreased the incidence and severity of GVHD. This observation is consistent with the transient presence of WJ-MSCs in recipients [49], as we could trace them only during the first 24 hours after injection. During this short period of time, we observed MSCs in the spleen, lungs and skin, and MSCs were in close contact with human PBMCs in the spleen. However, another group observed mitochondrial transfer in cord-blood MSCs and mouse (BALB/c) T cells from the spleen and mesenteric nodes[22]. In addition, xenogeneic GVHD in NSG mice was reduced by transplanting human PBMCs treated to artificially receive MSC-derived mitochondrial material[22]. Altogether, these data suggest that repeated injections of IFN-γ-primed WJ-MSCs better control GVHD than a single administration by allowing several short interactions between MSCs and activated T cells. Our data suggest that the synergistic effects of IDO and mitochondrial transfer on T-cell proliferation and metabolism observed *in vitro* may occur *in vivo*. Another mechanism of T-cell inhibition by human bone marrow-derived MSCs in an immunocompetent mouse model of GVHD has been described; alloreactive CD8 T lymphocytes transplanted into mice induced MSC apoptosis, and subsequent phagocytosis of apoptotic MSCs led to an increase in IDO activity[49]. Such a mechanism has never been described in an immunocompromised mouse model of GVHD but cannot be overlooking when discussing the beneficial effects of WJ-MSCS on GVHD. The relative implications of each mechanism will require further exploration.

Conclusions

In conclusion, our work reports for the first time that the synergistic interplay between IDO and contact-dependent mitochondrial transfer is required for WJ-MSCs to exert their immunosuppressive effects on activated T cells *in vitro*. We also show that IFN-γ priming, enhancing IDO activity, and 3 weekly injections of WJ-MSCs starting on Day 7 after HSC transplantation represent an optimized WJ-MSC treatment

regimen for GVHD prevention. Based on these results, we have set up a phase I trial (NCT05855707) including 3 administrations of IFN-γ-primed WJ-MSCs to prevent acute GVHD after haploidentical allogeneic HSCT.

Declarations

Ethics approval: This study requiring experimentation on mice was conducted after approval by the local Ethical Committee (CELMEA n°66), on 19th June 2018, under the following number APAFIS23270-2017060417575295-V10 (project entitled "immunomodulation of graft *versus* host disease by Wharton's Jelly mesenchymal stromal cells").

Consent for publication: Not applicable.

Availability of data and materials: The datasets during and/or analysed during the current study available from the corresponding author on reasonable request.

Competing interests:

Prof Danièle Bensoussan is a co-founder and member of the scientific advisory board of StemInov, a French Stem Cell company. She holds patent on the use of WJ-MSC for sepsis licensed to StemInov.

The other authors declare no competing interests.

Funding: This research received funding from the "Ligue contre le Cancer" Institute and the French Biomedicine Agency (ABM).

The authors would also like to sincerely thank the AREMIG and “Anaïs contre le cancer” associations for their support and their financial contribution to this research.

Authors’ contribution:

CP and RP carried out the experiments. AB, ABN, NC, MCB, GF, GC, and CV also helped carry out the experiments and interpret the results. PE and his team carried out the tryptophan metabolite assay. HS carried out the anatomopathology and immunohistochemistry analyses. CP, NI, MDA, and MTR wrote the manuscript. MTR, MDA, DM, MCB, DB and NI proofread and edited the manuscript.

References

1. Passweg JR, Baldomero H, Chabannon C, Basak GW, de la Cámara R, Corbacioglu S, et al. Hematopoietic cell transplantation and cellular therapy survey of the EBMT: monitoring of activities and trends over 30 years. Bone Marrow Transplant. 2021;56:1651–64.
2. Toubai T, Magenau J. Immunopathology and biology-based treatment of steroid-refractory graft-versus-host disease. Blood. 2020;136:429–40.

3. Zeiser R, von Bubnoff N, Butler J, Mohty M, Niederwieser D, Or R, et al. Ruxolitinib for Glucocorticoid-Refractory Acute Graft-versus-Host Disease. N Engl J Med. 2020;382:1800–10.
4. Bader P, Kuçi Z, Bakhtiar S, Basu O, Bug G, Dennis M, et al. Effective treatment of steroid and therapy-refractory acute graft-versus-host disease with a novel mesenchymal stromal cell product (MSC-FFM). Bone Marrow Transplant. 2018;53:852–62.
5. Bonig H, Kuçi Z, Kuçi S, Bakhtiar S, Basu O, Bug G et al. Children and Adults with Refractory Acute Graft-versus-Host Disease Respond to Treatment with the Mesenchymal Stromal Cell Preparation MSC-FFM-Outcome Report of 92 Patients. Cells. 2019;8.
6. Pochon C, Notarantonio A-B, Laroye C, Reppel L, Bensoussan D, Bertrand A, et al. Wharton's jelly-derived stromal cells and their cell therapy applications in allogeneic haematopoietic stem cell transplantation. J Cell Mol Med. 2022;26:1339–50.
7. Weiss ML, Anderson C, Medicetty S, Seshareddy KB, Weiss RJ, VanderWerff I, et al. Immune properties of human umbilical cord Wharton's jelly-derived cells. Stem Cells. 2008;26:2865–74.
8. Laroye C, Gauthier M, Antonot H, Decot V, Reppel L, Bensoussan D. Mesenchymal Stem/Stromal Cell Production Compliant with Good Manufacturing Practice: Comparison between Bone Marrow, the Gold Standard Adult Source, and Wharton's Jelly, an Extraembryonic Source. J Clin Med. 2019;8:E2207.
9. Pochon C, Laroye C, Kimmoun A, Reppel L, Dhuyser A, Rousseau H, et al. Efficacy of Wharton Jelly Mesenchymal Stromal Cells infusions in moderate to severe SARS-Cov-2 related acute respiratory distress syndrome: a phase 2a double-blind randomized controlled trial. Front Med (Lausanne). 2023;10:1224865.
10. Soder RP, Dawn B, Weiss ML, Dunavin N, Weir S, Mitchell J, et al. A Phase I Study to Evaluate Two Doses of Wharton's Jelly-Derived Mesenchymal Stromal Cells for the Treatment of De Novo High-Risk or Steroid-Refractory Acute Graft Versus Host Disease. Stem Cell Rev Rep. 2020;16:979–91.
11. Gao L, Zhang Y, Hu B, Liu J, Kong P, Lou S, et al. Phase II Multicenter, Randomized, Double-Blind Controlled Study of Efficacy and Safety of Umbilical Cord-Derived Mesenchymal Stromal Cells in the Prophylaxis of Chronic Graft-Versus-Host Disease After HLA-Haploidentical Stem-Cell Transplantation. J Clin Oncol. 2016;34:2843–50.
12. Wu Q-L, Liu X-Y, Nie D-M, Zhu X-X, Fang J, You Y, et al. Umbilical cord blood-derived mesenchymal stem cells ameliorate graft-versus-host disease following allogeneic hematopoietic stem cell transplantation through multiple immunoregulations. J Huazhong Univ Sci Technolog Med Sci. 2015;35:477–84.
13. Polchert D, Sobinsky J, Douglas G, Kidd M, Moadsiri A, Reina E, et al. IFN-gamma activation of mesenchymal stem cells for treatment and prevention of graft versus host disease. Eur J Immunol. 2008;38:1745–55.
14. Kim DS, Jang IK, Lee MW, Ko YJ, Lee D-H, Lee JW, et al. Enhanced Immunosuppressive Properties of Human Mesenchymal Stem Cells Primed by Interferon-γ. EBioMedicine. 2018;28:261–73.

15. D'Aveni M, Rossignol J, Coman T, Sivakumaran S, Henderson S, Manzo T, et al. G-CSF mobilizes CD34 + regulatory monocytes that inhibit graft-versus-host disease. Sci Transl Med. 2015;7:281ra42.
16. Blazar BR, Taylor PA, McElmurry R, Tian L, Panoskaltsis-Mortari A, Lam S, et al. Engraftment of severe combined immune deficient mice receiving allogeneic bone marrow via In utero or postnatal transfer. Blood. 1998;92:3949–59.
17. Laroye C, Lemarié J, Boufenzer A, Labroca P, Cunat L, Alauzet C, et al. Clinical-grade mesenchymal stem cells derived from umbilical cord improve septic shock in pigs. Intensive Care Med Exp. 2018;6:24.
18. Lefèvre A, Mavel S, Nadal-Desbarats L, Galineau L, Attucci S, Dufour D, et al. Validation of a global quantitative analysis methodology of tryptophan metabolites in mice using LC-MS. Talanta. 2019;195:593–8.
19. Argüello RJ, Combes AJ, Char R, Gigan J-P, Baaziz AI, Bousiquot E, et al. SCENITH: A Flow Cytometry-Based Method to Functionally Profile Energy Metabolism with Single-Cell Resolution. Cell Metab. 2020;32:1063–1075e7.
20. van Megen KM, van 't Wout E-JT, Lages Motta J, Dekker B, Nikolic T, Roep BO. Activated Mesenchymal Stromal Cells Process and Present Antigens Regulating Adaptive Immunity. Frontiers in Immunology [Internet]. 2019 [cited 2023 Oct 24];10. Available from: https://www.frontiersin.org/articles/10.3389/fimmu.2019.00694.
21. Wilfong EM, Croze R, Fang X, Schwede M, Niemi E, López GY et al. Proinflammatory cytokines and ARDS pulmonary edema fluid induce CD40 on human mesenchymal stromal cells—A potential mechanism for immune modulation. Zhao Y-Y, editor. PLoS ONE. 2020;15:e0240319.
22. Court AC, Le-Gatt A, Luz-Crawford P, Parra E, Aliaga-Tobar V, Bátiz LF, et al. Mitochondrial transfer from MSCs to T cells induces Treg differentiation and restricts inflammatory response. EMBO Rep. 2020;21:e48052.
23. Agrawal M, Rasiah PK, Bajwa A, Rajasingh J, Gangaraju R. Mesenchymal Stem Cell Induced Foxp3(+) Tregs Suppress Effector T Cells and Protect against Retinal Ischemic Injury. Cells. 2021;10:3006.
24. Sheng H, Wang Y, Jin Y, Zhang Q, Zhang Y, Wang L, et al. A critical role of IFNgamma in priming MSC-mediated suppression of T cell proliferation through up-regulation of B7-H1. Cell Res. 2008;18:846–57.
25. Wobma HM, Kanai M, Ma SP, Shih Y, Li HW, Duran-Struuck R, et al. Dual IFN-γ/hypoxia priming enhances immunosuppression of mesenchymal stromal cells through regulatory proteins and metabolic mechanisms. J Immunol Regen Med. 2018;1:45–56.
26. Prasanna SJ, Gopalakrishnan D, Shankar SR, Vasandan AB. Pro-inflammatory cytokines, IFNgamma and TNFalpha, influence immune properties of human bone marrow and Wharton jelly mesenchymal stem cells differentially. PLoS ONE. 2010;5:e9016.
27. He H, Nagamura-Inoue T, Takahashi A, Mori Y, Yamamoto Y, Shimazu T, et al. Immunosuppressive properties of Wharton's jelly-derived mesenchymal stromal cells in vitro. Int J Hematol.

2015;102:368–78.

28. Li X, Xu Z, Bai J, Yang S, Zhao S, Zhang Y, et al. Umbilical Cord Tissue-Derived Mesenchymal Stem Cells Induce T Lymphocyte Apoptosis and Cell Cycle Arrest by Expression of Indoleamine 2, 3-Dioxygenase. Stem Cells Int. 2016;2016:7495135.
29. Wang D, Feng X, Lu L, Konkel JE, Zhang H, Chen Z, et al. A CD8 T cell/indoleamine 2,3-dioxygenase axis is required for mesenchymal stem cell suppression of human systemic lupus erythematosus. Arthritis Rheumatol. 2014;66:2234–45.
30. Burnham AJ, Foppiani EM, Horwitz EM. Key Metabolic Pathways in MSC-Mediated Immunomodulation: Implications for the Prophylaxis and Treatment of Graft Versus Host Disease. Front Immunol. 2020;11:609277.
31. Wang G, Cao K, Liu K, Xue Y, Roberts AI, Li F, et al. Kynurenic acid, an IDO metabolite, controls TSG-6-mediated immunosuppression of human mesenchymal stem cells. Cell Death Differ. 2018;25:1209–23.
32. Eleftheriadis T, Pissas G, Antoniadi G, Liakopoulos V, Stefanidis I. Indoleamine 2,3-dioxygenase depletes tryptophan, activates general control non-derepressible 2 kinase and down-regulates key enzymes involved in fatty acid synthesis in primary human CD4 + T cells. Immunology. 2015;146:292–300.
33. Metz R, Rust S, Duhadaway JB, Mautino MR, Munn DH, Vahanian NN, et al. IDO inhibits a tryptophan sufficiency signal that stimulates mTOR: A novel IDO effector pathway targeted by D-1-methyl-tryptophan. Oncoimmunology. 2012;1:1460–8.
34. Böttcher M, Hofmann D, Bruns A, Haibach H, Loschinski M, Saul R. Mesenchymal Stromal Cells Disrupt mTOR-Signaling and Aerobic Glycolysis During T-Cell Activation. Stem Cells. 2016;34:516–21.
35. Eleftheriadis T, Pissas G, Sounidaki M, Tsogka K, Antoniadis N, Antoniadi G, et al. Indoleamine 2,3-dioxygenase, by degrading L-tryptophan, enhances carnitine palmitoyltransferase I activity and fatty acid oxidation, and exerts fatty acid-dependent effects in human alloreactive CD4 + T-cells. Int J Mol Med. 2016;38:1605–13.
36. Siska PJ, Jiao J, Matos C, Singer K, Berger RS, Dettmer K, et al. Kynurenine induces T cell fat catabolism and has limited suppressive effects in vivo. EBioMedicine. 2021;74:103734.
37. Spees JL, Olson SD, Whitney MJ, Prockop DJ. Mitochondrial transfer between cells can rescue aerobic respiration. Proc Natl Acad Sci U S A. 2006;103:1283–8.
38. Jackson MV, Morrison TJ, Doherty DF, McAuley DF, Matthay MA, Kissenpfennig A, et al. Mitochondrial Transfer via Tunneling Nanotubes is an Important Mechanism by Which Mesenchymal Stem Cells Enhance Macrophage Phagocytosis in the In Vitro and In Vivo Models of ARDS. Stem Cells. 2016;34:2210–23.
39. Chu PPY, Bari S, Fan X, Gay FPH, Ang JML, Chiu GNC, et al. Intercellular cytosolic transfer correlates with mesenchymal stromal cell rescue of umbilical cord blood cell viability during ex vivo expansion. Cytotherapy. 2012;14:1064–79.

40. Mohammadalipour A, Dumbali SP, Wenzel PL. Mitochondrial Transfer and Regulators of Mesenchymal Stromal Cell Function and Therapeutic Efficacy. Front Cell Dev Biol. 2020;8:603292.
41. Feng Y, Zhu R, Shen J, Wu J, Lu W, Zhang J, et al. Human Bone Marrow Mesenchymal Stem Cells Rescue Endothelial Cells Experiencing Chemotherapy Stress by Mitochondrial Transfer Via Tunneling Nanotubes. Stem Cells Dev. 2019;28:674–82.
42. Plotnikov EY, Khryapenkova TG, Vasileva AK, Marey MV, Galkina SI, Isaev NK, et al. Cell-to-cell cross-talk between mesenchymal stem cells and cardiomyocytes in co-culture. J Cell Mol Med. 2008;12:1622–31.
43. Tseng N, Lambie SC, Huynh CQ, Sanford B, Patel M, Herson PS, et al. Mitochondrial transfer from mesenchymal stem cells improves neuronal metabolism after oxidant injury in vitro: The role of Miro1. J Cereb Blood Flow Metab. 2021;41:761–70.
44. Jiang D, Gao F, Zhang Y, Wong DSH, Li Q, Tse H-F, et al. Mitochondrial transfer of mesenchymal stem cells effectively protects corneal epithelial cells from mitochondrial damage. Cell Death Dis. 2016;7:e2467.
45. Do J-S, Zwick D, Kenyon JD, Zhong F, Askew D, Huang AY, et al. Mesenchymal stromal cell mitochondrial transfer to human induced T-regulatory cells mediates FOXP3 stability. Sci Rep. 2021;11:10676.
46. Vallabhaneni KC, Haller H, Dumler I. Vascular smooth muscle cells initiate proliferation of mesenchymal stem cells by mitochondrial transfer via tunneling nanotubes. Stem Cells Dev. 2012;21:3104–13.
47. Levoux J, Prola A, Lafuste P, Gervais M, Chevallier N, Koumaiha Z, et al. Platelets Facilitate the Wound-Healing Capability of Mesenchymal Stem Cells by Mitochondrial Transfer and Metabolic Reprogramming. Cell Metab. 2021;33:283–299e9.
48. Ahmad T, Mukherjee S, Pattnaik B, Kumar M, Singh S, Kumar M, et al. Miro1 regulates intercellular mitochondrial transport & enhances mesenchymal stem cell rescue efficacy. EMBO J. 2014;33:994–1010.
49. Galleu A, Riffo-Vasquez Y, Trento C, Lomas C, Dolcetti L, Cheung TS, et al. Apoptosis in mesenchymal stromal cells induces in vivo recipient-mediated immunomodulation. Sci Transl Med. 2017;9:eaam7828.

Figures

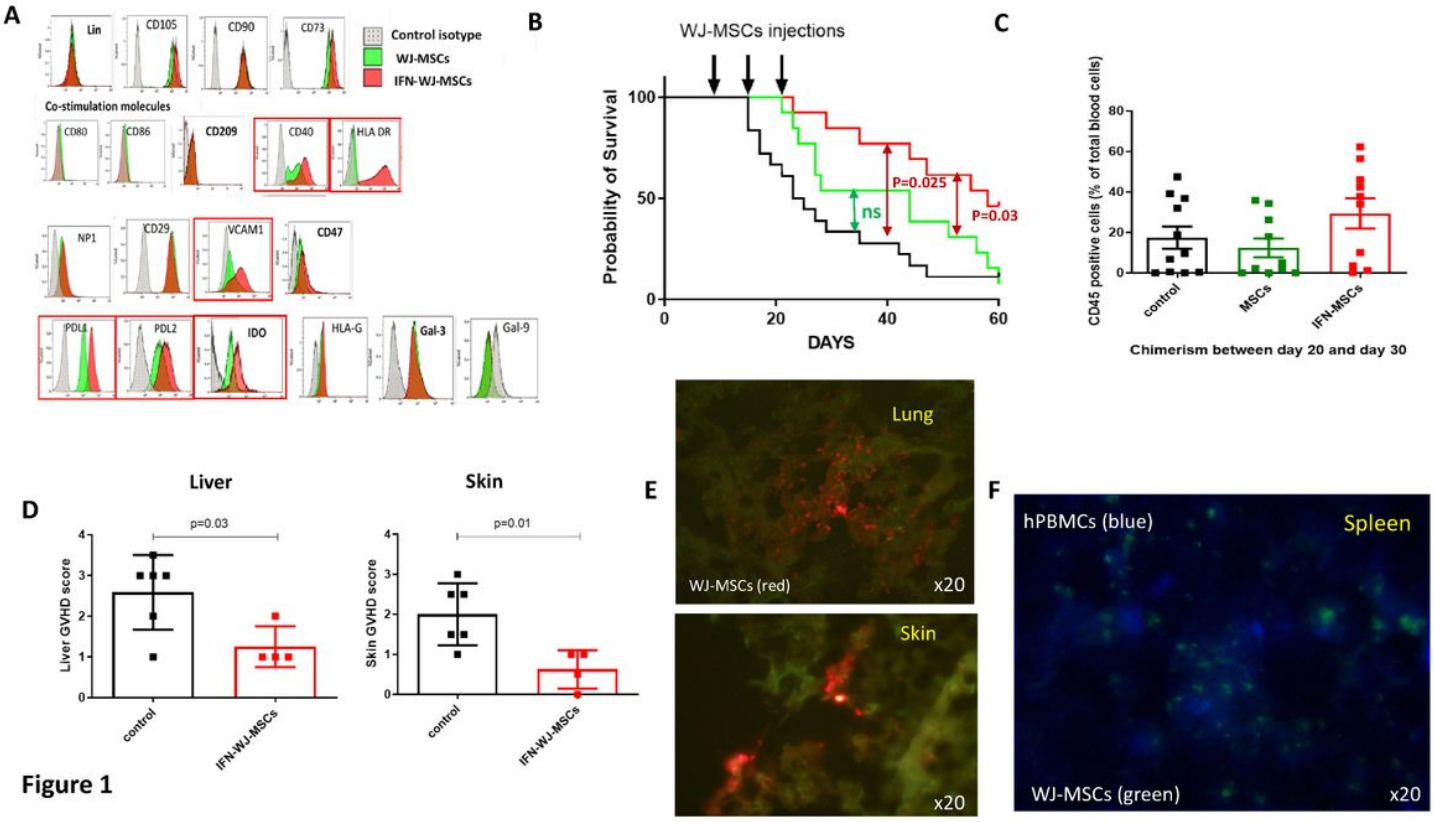

Figure 1

Figure 1

IFN-WJ-MSCs decrease mice mortality from GVHD and transiently colocalize with T cells in spleen

A. *Flow cytometry analysis on cell surface or intracellular markers of WJ-MSCs (green) versus IFN-WJ-MSCs (red).* ***B.*** *NSG mice were irradiated at 2 grays on day -1 and transplanted intravenously with $5x10^6$ human PBMCs on day 0 alone (PBS group, blue curve, n=19) or associated with sequential administration of $5x10^5$ WJ-MSCs (green curve, n=15) or of IFN-WJ-MSCs (red curve, n=13) on days 7, 14, and 21 post-transplantation.* ***C.*** *Human CD45+ cell chimerism was evaluated by flow cytometry between day 20 and 30 in the 3 transplanted groups. Human CD45+ cells are represented as percentages of all viable targeted cells.* ***D****. Reduction of GVHD scores in the skin (left) and liver (right) between mice transplanted with human PBMCs alone (PBS control group, n=6) and those having received IFN-WJ-MSCs (n=4).* ***E.*** *IFN-WJ-MSCs were stained with Celltracker™ Deep Red Dye. IFN-WJ-MSCs were detected in clusters 24hours after their injection in the lungs (**Up**) and the skin (**Down**).* ***F.*** *Human PBMCS were stained with Celltracker blue, ThermoFisher, 24 hours before their injection in mice. IFN-WJ-MSCs were doubly stained with Mitotracker Green.*

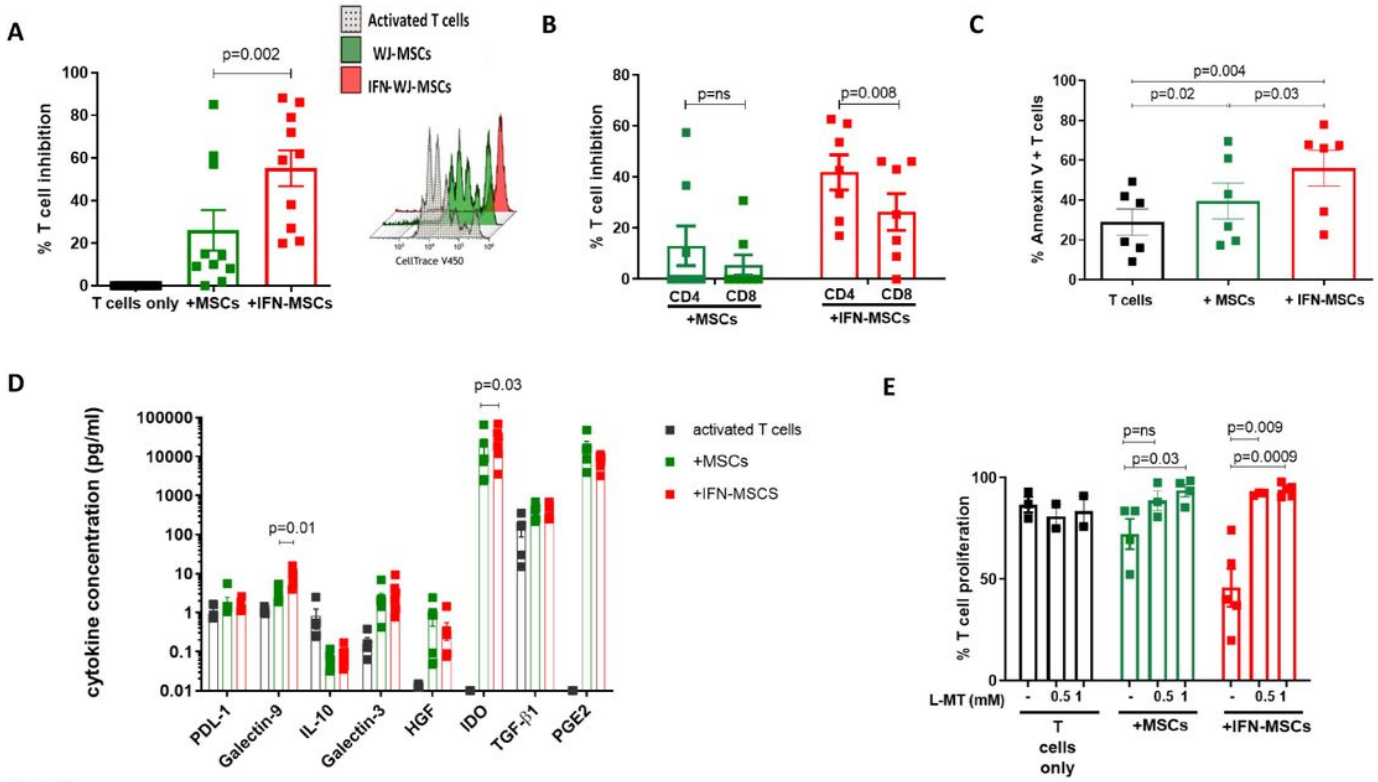

Figure 2

Figure 2

IFN-WJ-MSCs display higher immune suppressive potential, reversed by IDO inhibition

A.*Increased inhibition of CD3/CD28 activated CD3+ T cell proliferation after 5 days of co-culture with IFN-WJ-MSCs (red) versus WJ-MSCs (green) (n=10 different cord sources). Right: Illustration of T cell proliferation assessed by the dilution of Celltrace after 5 days of stimulation by anti-CD3/CD28 mAbs alone (grey) or in the presence of IFN-WJ-MSCs (red) and WJ-MSCs (green).* ***B.*** *Comparison of T cell proliferation inhibition on activated CD4+ vs CD8+ T cell subtypes after co-cultures with WJ-MSCs (green) and IFN-WJ-MSCs (red) (n=7).* ***C.*** *Increased T cell apoptosis, analyzed by flow cytometry with Annexin V staining, after 2 days of CD3/CD28 activation in the presence of WJ-MSCs (green) and of IFN-WJ-MSCs (red) in comparison to activated T cells alone (white) (n=6)=* ***D.*** *Comparison of the indicated cytokines' concentrations measured by single and multiplex Elisa in the supernatants on day 5 of culture of CD3/CD28 activated T cells alone (grey) or with WJ-MCS (green) or IFN-γ-WJ-MSCs (red) (n=6 independent co-cultures).* ***E.*** *Addition of the IDO inhibitor 1L-MT at the beginning of co-cultures between CD3/CD28 activated T cells and unprimed or IFN-γ-primed WJ-MSCs fully abrogated the immunosuppressive effects of both WJ-MSCs and IFN-WJ-MSCs (n=6 co-cultures with 5 different cord sources).*

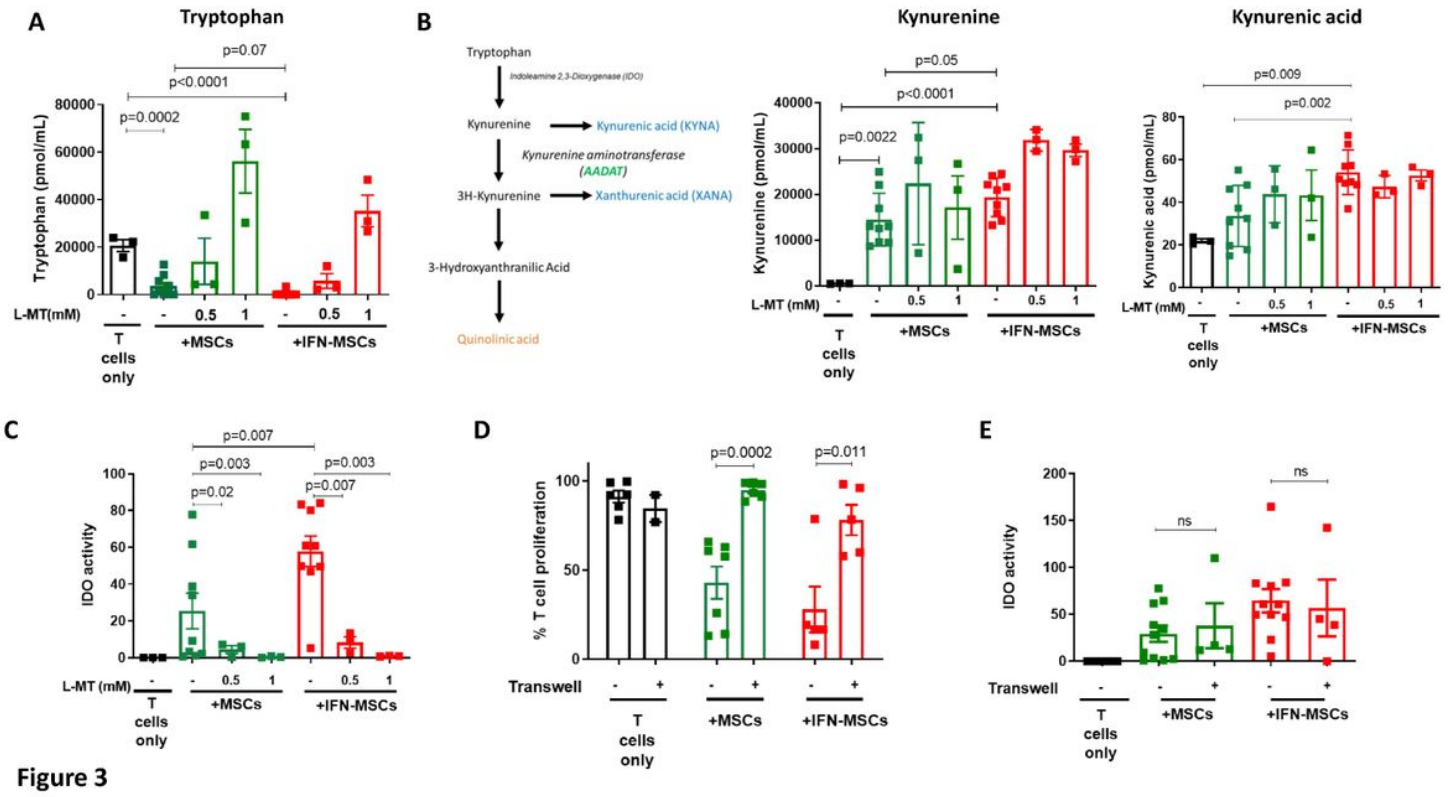

Figure 3

Figure 3

IDO activity is a key mechanism of WJ-MSCs immunosuppression

A, B, C. *Concentrations of Tryptophan (A) and its metabolites Kynurenine (B) and Kynurenic acid (C) were measured in the supernatants on day 5 of culture of CD3/CD28 activated T cells alone (grey) or with WJ-MCS (green) or IFN-γ-WJ-MSCs (red) (n=6) in the presence or not of 1L-MT at 0.5 mM and 1mM (n=3).* ***A. B. Left****: Schematic diagram of the tryptophan degradation pathway via IDO.* ***Middle****: Kynurenic acid concentrations were only increased in co-cultures with IFN-WJ-MSCs* ***Right****: Kynurenine concentrations were higher in co-cultures with both WJ-MSCs and IFN-WJ-MSCs.* ***C****. IDO activity was evaluated by the ratio of tryptophan metabolites depending on IDO (kynurenine + kynurenic acid + 3OH-kynurenine + quinolinic acid + xanthurenic acid) to tryptophan metabolites that do not depend on IDO (tryptophan + 5OH-tryptophan + tryptamine + serotonin + tryptophol).* ***D.*** *The impact of cell-contact on the suppressive effects of WJ-MSCS (green) and IFN-WJ-MSCs (red) was analyzed using a transwell separating CD3/CD28 activated T cells from MSCs during the co-culture (n=5 to 7).* ***E.*** *Evaluation of IDO activity from metabolites measured in the culture supernatants on day 5 of co-cultures between CD3/CD28 activated T cells alone or with WJ-MSCS and IFN-WJ-MSCs (n=4).*

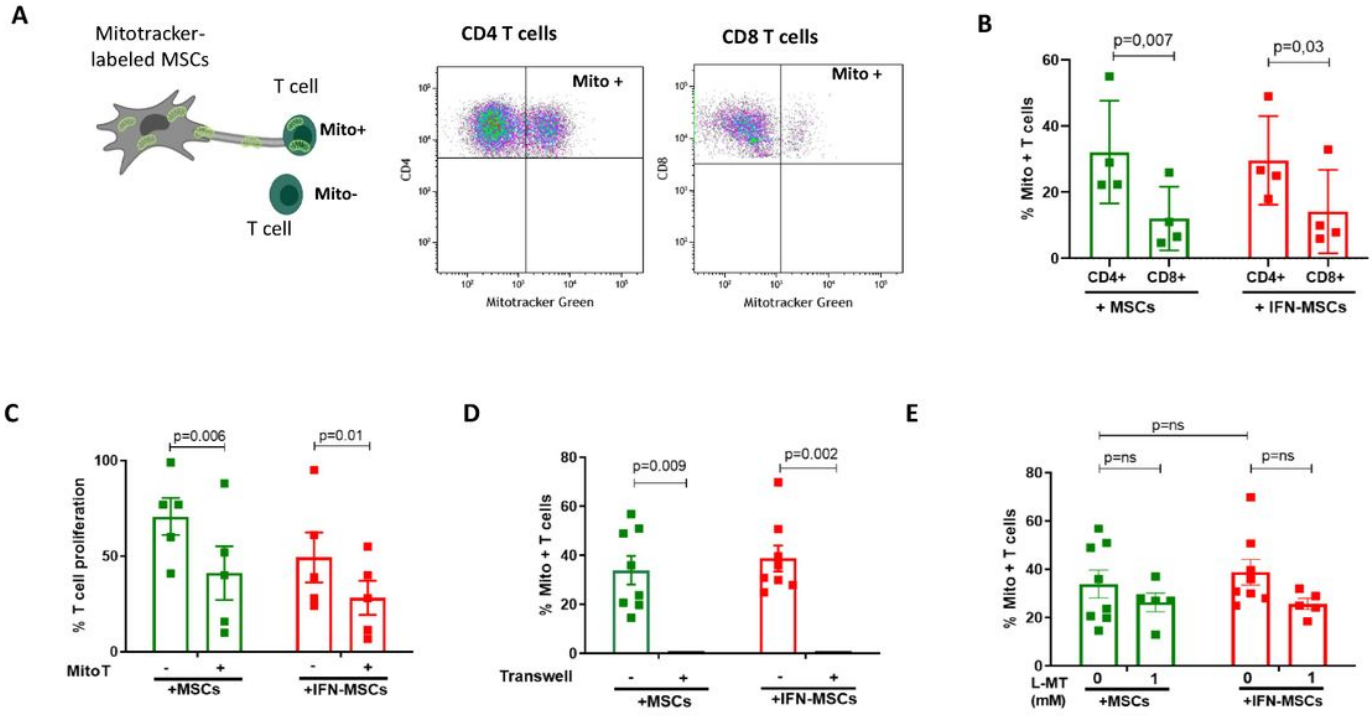

Figure 4

Figure 4

Mitochondrial transfer is another key mechanism

A. *Mitochondrial transfer from WJ-MSCs to activated CD4+ T cells and CD8+ Tcells was analyzed by flow cytometry using a mitotracker, that labelled WJ-MSCs mitochondria before T/WJ-MSCs co-culture. Cytometry dot plots illustrating mitochondrial transfer to CD4+ and CD8+ T cells.* ***B.*** *CD4+ T cells received mitochondria from WJ-MSCs and IFN-WJ-MSCs at a higher percentage than CD8+ T cells (n=4).* ***C.*** *Proliferation of CD3/CD28 Mito+ and Mito- CD4 + T cells was evaluated after 5 days of culture with WJ-MSCs and IFN-WJ-MSCs (n=5).* ***D.*** *Mitochondrial transfer from WJ-MSCs and IFN-WJ-MSCs to activated CD4+ T cells was analyzed in co-cultures with (n=3) or without transwells (n=8).* ***E.*** *Inhibition of IDO by 1L-MT did not significantly change the rate of mitochondrial transfer from WJ-MSCs or IFN-WJ-MSCs to activated CD4+ T cells (n=4).*

Figure 5

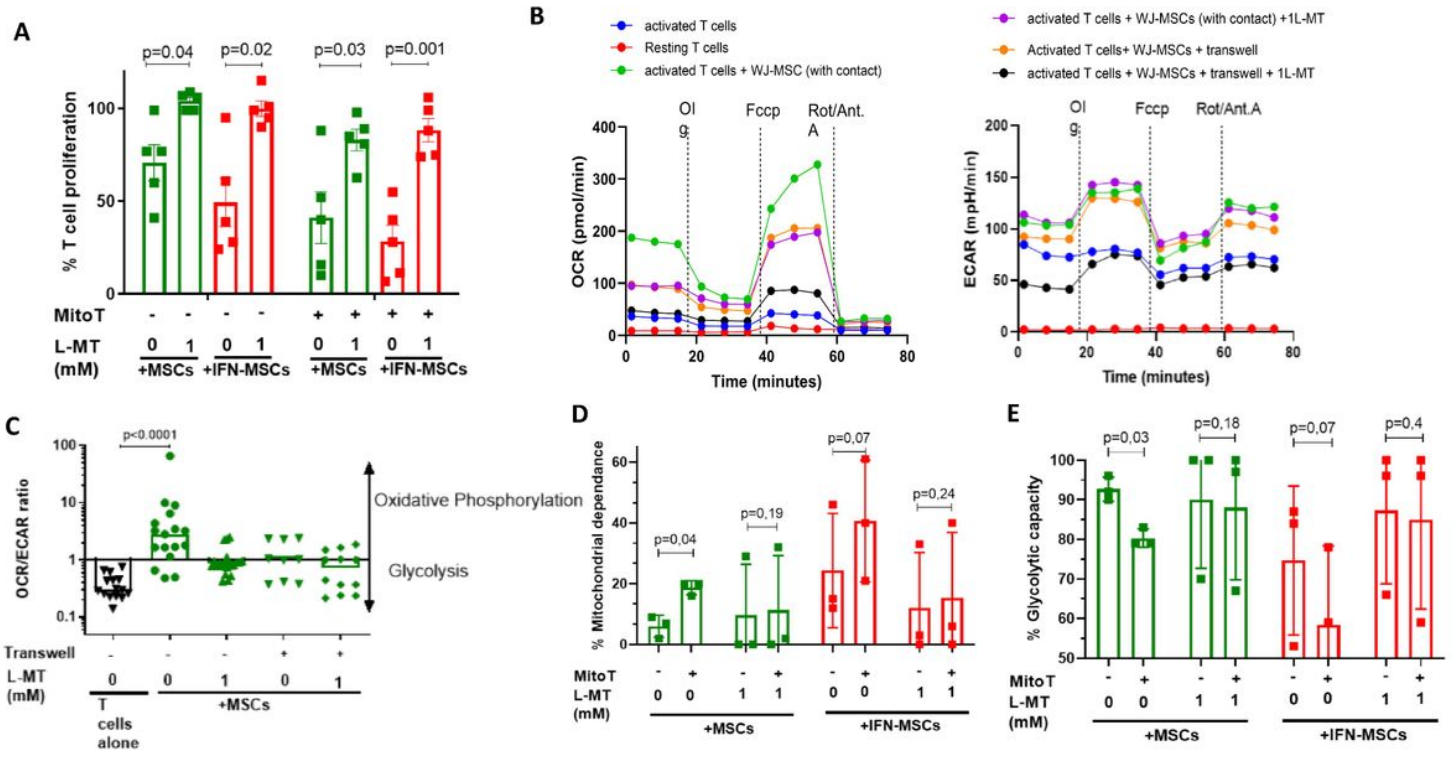

Figure 5

Mitochondrial transfer and IDO act synergistically to induce a metabolic shift in T cells from glycolysis to oxidative phosphorylation

A.*IDO inhibition (by 1L-MT at 1 mM) restored the proliferation of activated mito+ and mito - T cells co-cultured with WJ-MSCs and IFN-WJ-MSCs for CD4+ T cells (n=5).* ***B.*** *T cell metabolism was analyzed by Seahorse in the different culture conditions: resting and CD3/CD28 activated T cells with or without WJ-MSCs with or without transwell and/or 1L-MT (n=4).* ***Left:*** *OCR curves are shown for all conditions mentioned (1 representative experiment, reproduced 4 times).* ***Right:*** *ECAR curves for all conditions mentioned (1 representative experiment, reproduced 4 times).* ***C.*** *Analysis of OCR/ECAR ratio in the different conditions mentioned above (n=4).* ***D, E.*** *T cell metabolism was analyzed with Scenith technology, according to their status Mito+ and Mito- (Mito+ T cells were gated by cytometry thanks to their fluorescent mitotracker) (n=3).* ***D.*** *Mitochondrial dependence was superior in Mito + T cells after their co-culture with WJ-MSCs by comparison to Mito- T cells* ***E.*** *Gycolytic capacity was inferior in Mito + T cells after their co-culture with WJ-MSCs by comparison to Mito- T cells.*

Supplementary Files

This is a list of supplementary files associated with this preprint. Click to download.

- AuthorChecklistFull.pdf

- SupplementaryFigure1.pptx
- SupplementaryFigure2.pptx